SEMIQUANTITATIVE CHEMICAL ANALYSIS OF ASBESTOS FIBERS AND CLAY MINERALS WITH AN ANALYTICAL ELECTRON MICROSCOPE

Hisato Hayashi

Research Institute of Underground Resources, Mining College,
Akita University, Akita 010, Japan

Saburo Aita and Mikio Suzuki

Application Department, JEOL Ltd., Nakagami, Akishima 196, Japan

(Received 31 May 1977)

Abstract—By using a transmission electron microscope equipped with an energy dispersive spectrometer, it was possible to detect the morphological, structural, and chemical characteristics of individual asbestos fibers and clay minerals without any realignment of the equipment. A rapid and convenient procedure for semiquantitative analysis is proposed. Analyses are given for 21 hydrous silicates, asbestos and clay minerals, by both ordinary chemical and energy dispersive methods. The energy dispersive results were comparable to those obtained by chemical analysis. Application of this procedure to asbestos fibers proved this method to be practical and valid for characterization of asbestos in environmental and tissue samples.

Key Words—Amphibole, Asbestos, Chrysotile, Morphology, Structure.

INTRODUCTION

Energy dispersive analysis of X-rays in the transmission electron microscope has emerged during the past few years as a highly useful analytical technique in a variety of research fields such as air pollution, pathology, forensic chemistry, and experimental petrology. This technique has enabled the compositional determination of individual microparticles of less than 1 μm^3. Electron microprobe analysis of major elements in bulk samples has been described by a number of authors. The analytical techniques for bulk specimens are inapplicable to X-ray microanalysis of ultrathin specimens in the electron microscope, because the characteristic X-ray intensity depends on the thickness of the specimen as well as on the chemical composition. The effect of the specimen thickness on the characteristic X-ray intensity was eliminated by Marshall and Hall (1968). They showed that the intensity ratio of a characteristic peak to the intensity of the continuum provides a measure for the concentration of an element, which is independent of the film thickness. Literature exists on application of the analytical electron microscope to environmental and tissue samples whose volumes of less than 1 μm^3 (Langer et al., 1971, 1974; Pooley, 1972, 1976; Henderson et al., 1973; Rubin and Maggiore, 1974); but few of these investigations have determined chemical components quantitatively for silicate minerals, especially submicron particles.

Asbestos has been studied in the field of occupational health in relation to respiratory disease as well as pleural cancer (Selikoff, 1972). Recently the contamination of public water supplies by fibrous amphibole minerals was found in tailing discharge of an iron ore mining company located in Minnesota (Nicholson, 1974; Kramer, 1976). In order to monitor these health effects and the extent of environmental contamination by asbestos, the identification and characterization of microparticles have become important fields of study. Asbestos fibers have been intensively studied for these reasons.

This study is initiated to use the analytical electron microscope for the semiquantitative determination of the major elements in 21 hydrous silicate minerals which already have been analyzed by ordinary chemical methods.

SPECIMENS AND METHOD

Specimens used in this study are listed in Table 1. These minerals were confirmed to be pure minerals by X-ray, thermal, and chemical analyses.

The analytical electron microscope is composed of the JEM-100 C type transmission electron microscope, EM-SEG side entry goniometer, EM-ASID high resolution scanning attachment, and EM-NDS dispersive X-ray spectrometer. The instrument was operated at 40 kV.

The particles of each specimen were deposited from suspension on a supporting film on an electron microscope grid, and then coated with carbon. The isolated particles were selected on the STEM image, and then analyzed using the EM-NDS dispersive X-ray spectrometer.
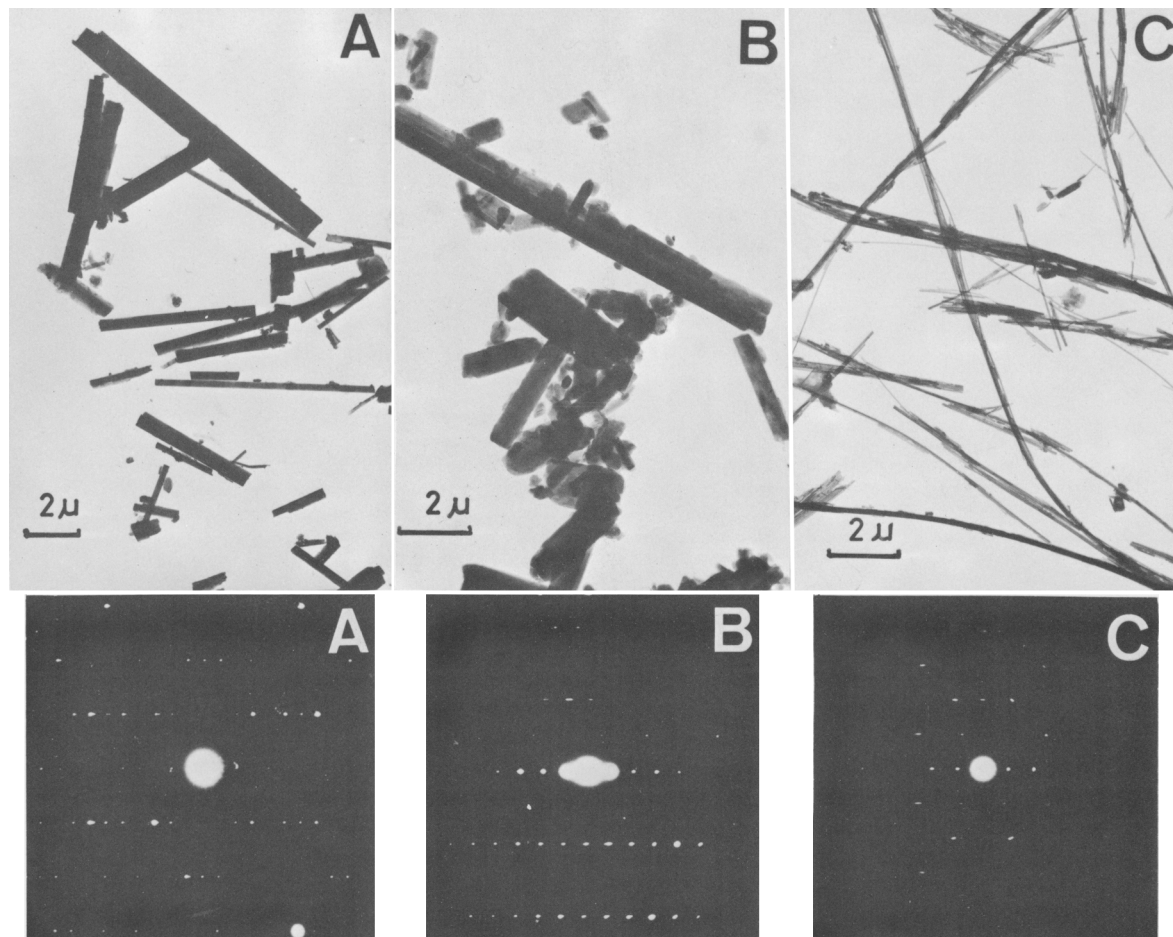
Fig. 1. Transmission electron micrographs and selected area diffraction patterns obtained on amosite (A), crocidolite (B) and chrysotile (C).

Table 1. Details of analyzed minerals.

| No.	Minerals	Locality	Ref. No.	Analyst	
1	Chrysotile	Cassier mine, Canada.	Cassier AA	Hayashi	(1971)
2	Chrysotile	Yamabe mine, Hokkaido, Japan.		Hayashi	(1971)
3	Anthophyllite	South America.		Komuro	(1975)
4	Anthophyllite	Unknown.		Hayashi	(1971)
5	Amosite	Penge mine, South Africa.	A-10	Hayashi	(1971)
6	Amosite	Penge mine, South Africa.	S-22	Hayashi	(1971)
7	Tremolite	Sue-machi, Fukuoka, Japan.		Komuro	(1975)
8	Tremolite	Iwate, Japan.		Komuro	(1975)
9	Actinolite	Sekikawa-mura, Ehime, Japan.		Komuro	(1975)
10	Actinolite	Ohgushi, Nagasaki, Japan.		Hayashi	(1971)
11	Crocidolite	Kuruman mine. South Africa.	M	Hayashi	(1971)
12	Crocidolite	Kuruman mine, South Africa.	J-10	Hayashi	(1971)
13	Halloysite	Kusatsu, Gunma, Japan.		Sato	(1968)
14	Pyrophyllite	Honami mine, Nagano, Japan.	H-2	Kodama	(1958)
15	Talc	Haicheng, China.		Komuro	(1974)
16	Sepiolite	Kuzuu, Tochigi, Japan.		Nakamura	(1966)
17	Palygorskite	Kuzuu, Tochigi, Japan.		Nakamura	(1968)
18	Al-chlorite	Kamikita mine, Aomori, Japan.	K-40	Hayashi	(1964)
19	Al-Mg-chlorite	Hanaoka mine, Akita, Japan.	H-330	Hayashi	(1961)
20	Mg-chlorite	Wanibichi mine, Shimane, Japan.		Sudo	(1956)
21	Fe-chlorite	Ichinokoshi, Toyama, Japan.		Sudo	(1943)
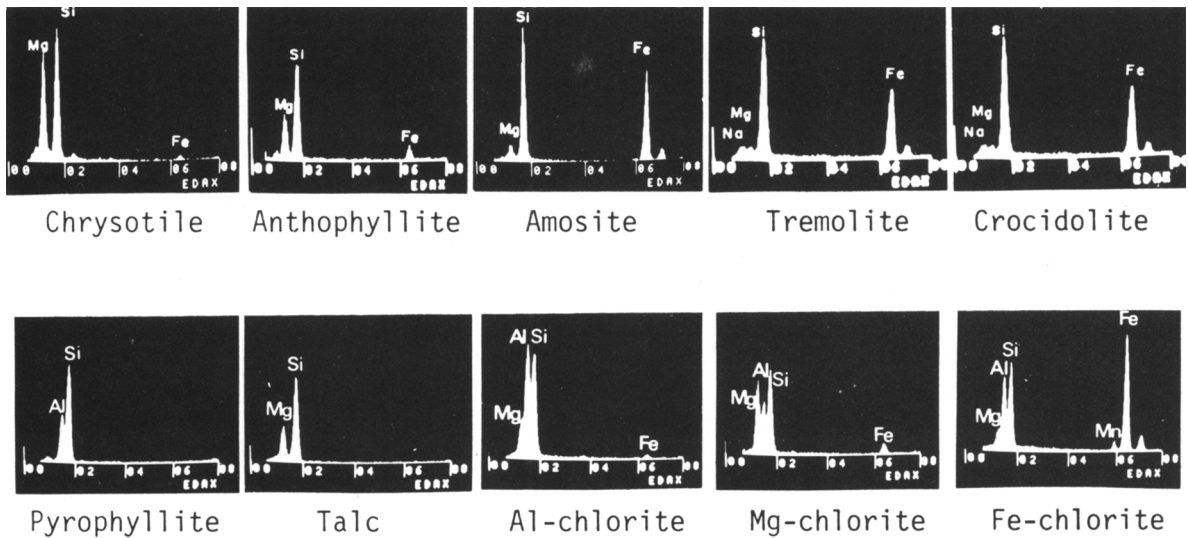
Fig. 2. Energy dispersive spectrometer spectra for various asbestos fibers and clay minerals.

EXPERIMENTAL RESULTS

Asbestos and related minerals

The asbestos minerals are natural, hydrated silicates which occur as fibers. Asbestos fibers are classified into two groups: amphiboles and chrysotile. Anthophyllite, amosite, tremolite, actinolite and crocidolite belong to the amphibole mineral in which cations link the infinite chains of composition $Si_8O_{22}(OH)_2$. As shown in Figure 1, each fiber of amphibole asbestos tends to form straight edges parallel to the fiber axis and vary from electron-dense fibers to opaque ones. On the other hand, chrysotile fibrils normally consist of a central capillary and electron opaque walls.

Chrysotile yields a unique selected area electron diffraction pattern as shown in Figure 1. Layer lines which denote the periodicity of the fiber axis a yield measurements of 5.3 Å. Figure 1 also shows two representative selected area electron diffraction patterns of amphibole asbestos which are quite different from that of chrysotile. Amphiboles, however, are quite similar in diffraction patterns (Figure 1). It is difficult to distinguish a particular mineral species among amphiboles, because these diffraction patterns resemble each other. This technique, however, is very effective for differentiating chrysotile from amphibole asbestos.

X-ray emission spectra of five asbestiform minerals are shown in Figure 2. Chrysotile shows two large peaks for silicon and magnesium, and a small peak for iron. As can be seen, chrysotile and anthophyllite have similar spectra but they differ in relative amounts of magnesium, silicon and iron. Amosite has two large peaks for silicon and iron, and a small peak for magnesium. Tremolite, on the other hand, differs significantly from the above-mentioned three minerals due to the presence of a calcium peak. The presence of a sodium peak in crocidolite is one of the most notable differences among the six species of asbestiform minerals.

Chrysotile is the trioctahedral analogue of the kaolin minerals and shows certain morphological similarities to halloysite. Halloysite fibers are generally difficult to distinguish from chrysotile fibrils, but X-ray emission spectra can show easily the difference in chemistry of these minerals.

Clay minerals

Talc, pyrophyllite, sepiolite, palygorskite and four kinds of chlorites were examined with the analytical electron microscope. Talc and pyrophyllite were difficult to identify from their morphology or from their electron diffraction patterns. The tetrahedral cation population of talc and pyrophyllite is mainly silicon and the octahedral sheet contains aluminum in pyrophyllite and magnesium in talc. Therefore X-ray energy spectra for talc show a large silicon peak and a peak for magnesium while that for pyrophyllite has a large peak for silicon and an aluminum peak (Figure 2).

The sepiolite-palygorskite group is a series of hydrous magnesium minerals. Palygorskite is the aluminum- or iron-rich member and sepiolite is the aluminum-poor member. The electron micrographs of these minerals have revealed that the particles consist of elongated fibers which are axially parallel, sharp-edged and unevenly broken at their ends. The predominant peaks in the energy dispersive X-ray spectra are magnesium and silicon for the sepiolite fiber, and silicon, aluminum and magnesium from the palygorskite fiber.

The chlorites are a group of hydrous silicate minerals whose structure permits extensive isomorphous substitution. These minerals vary in chemical composition

Table 2. Results of energy dispersive analysis (e) compared with chemical analysis (c). Wt % oxides.

NO.		SiO_2	TiO	Al_2O_3	Fe_2O_3	FeO	Total Fe	MnO	MgO	CaO	K_2O	Na_2O	Cr_2O_5	P_2O_5	total	H_2O (+)	H_2O (-)	Total
1	e	41.44	-	0.95	2.24	0.15	2.84	0.07	34.44	0.11	3.78	0.03	0.10	-	82.50	12.77	0.98	99.64
	c	40.85					2.41*		41.38		0.01				85.89			
2	e	43.00	-	2.02	0.61	2.67	6.44	0.10	33.13	0.06	2.55	0.48	-	-	85.12	14.11	0.55	99.98
	c	39.06					3.27**		40.16		0.16				85.32			
3	e	61.54	0.08	1.51	1.60	4.30	3.70	0.05	25.79	-	0.01	0.05	-	0.01	92.54	6.03	1.09	99.67
	c	54.40		1.15			5.88**		30.90						92.55			
4	e	57.91	0.69	6.01	3.75	0.63	6.00	-	27.25	1.10	1.34	0.10	0.23	-	98.74	1.08	0.55	100.40
	c	56.52		5.60			4.45*		30.33		0.05				98.77			
5	e	51.22	0.04	1.45	3.00	32.17	35.27	0.32	8.70	0.52	0.32	0.10			95.19	4.49	0.23	99.94
	c	51.35					35.14**		5.95						95.22			
6	e	54.77	C.16	1.39	2.78	36.68	35.73	1.37	5.73	0.42	0.02	0.04		-	97.60	2.64	0.06	100.34
	c	49.11					39.43**	0.96	6.08						97.64			
7	e	59.80	0.03	1.55	-	2.03	0.66	0.06	19.69	17.04	0.01	0.07		0.01	97.26	2.40	0.09	99.75
	c	57.30					2.03		23.70	12.50					97.26			
8	e	55.83	0.07	2.86	0.36	4.76	2.81	0.17	18.17	17.31	0.04	0.05		0.01	96.98	2.53	0.23	99.75
	c	55.80		1.63			5.12**		21.20	12.90					96.99			
9	e	59.56	0.10	3.64	0.49	5.96	5.15	0.21	16.65	13.14	0.05	0.52		0.01	98.14	1.69	0.00	99.86
	c	56.40		2.53			6.45**		20.10	11.80					98.17			
10	e	57.87	-	4.18	0.76	4.08	4.34	0.27	18.54	12.72	0.21	0.21			97.65	2.18	0.16	100.06
	c	55.17		4.37			4.83**		21.38	11.27					97.72			
11	e	58.77	0.03	0.49	17.81	18.46	30.44	0.05	3.52	0.91	0.09	4.26		-	96.99	3.04	0.39	100.41
	c	50.21					36.09**		3.35			5.63			97.03			
12	e	52.97	0.13	3.97	17.42	18.48	28.00	0.05	5.25	0.84	0.07	5.76		-	95.95	3.29	0.34	99.68
	c	49.34		0.52			35.73**		3.44			5.76			96.05			
13	e	45.67	-	36.29	1.33	0.32	1.69*	-	0.20	0.09	none	none		-	81.96	14.80	2.90	99.69
	c	43.64		36.41											81.99			
14	e	64.80	0.09	29.78	0.16	0.08	0.25*	none	0.45	0.12	tr.	0.01		tr.	94.58	5.45	0.84	100.82
	c	64.02		29.60											94.53			
15	e	66.16	-	-	0.04		0.04	-	28.81	-	0.01	0.02	-	0.10	94.97	5.27	0.07	100.33
	c	64.50							30.32						94.99			
16	e	54.10	-	1.03	0.04	0.01	0.05	0.01	24.07	0.51	-	-	-	-	78.17	9.04	12.67	99.90
	c	52.85							23.74						78.19			
17	e	51.32	-	13.52	1.83	0.26	1.63	none	8.35	3.95	0.02	tr.	-	-	78.77	12.04	10.16	99.97
	c	53.75		10.23			2.12*		9.39	2.29					77.77			
18	e	35.03	-	35.27	5.01	0.43	3.34	0.05	12.64	1.13	0.46	0.24		-	86.28	12.24	1.91	100.60
	c	35.63		34.87			5.49*		8.63						86.45			
19	e	36.16	0.36	23.04	0.15	0.03	3.52	-	21.20	1.08	0.01	0.14		-	83.92	13.56	1.75	99.28
	c	30.02		30.74			0.18*		21.44						83.97			
20	e	29.79	0.32	23.56	0.83	3.67	2.99	-	29.40	C.19	-	-		-	85.74	10.76	2.76	99.32
	c	29.07		21.82			4.49**		29.90						85.80			
21	e	23.07	-	19.49	13.38	26.26	25.53	2.70	6.27	-	3.90	-	5.21 (C1)		86.17	10.05	0.98	99.48
	c	22.24		17.05			39.51**	5.42	4.10						88.45			

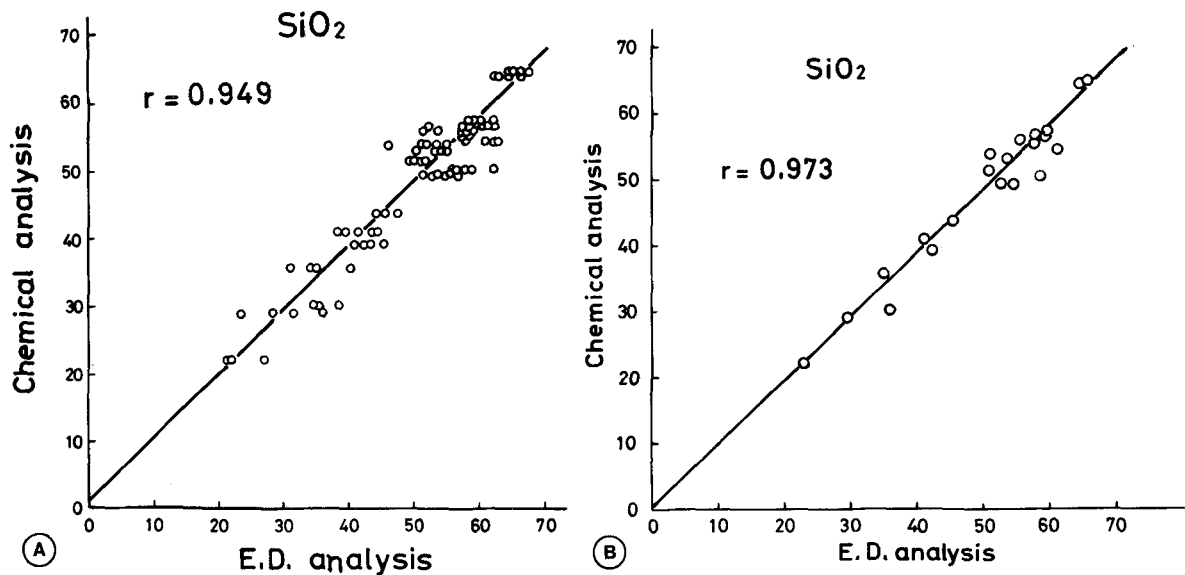Note : * indicates ferrous oxide + ferric oxide x 0.99 ; ** indicates ferrous oxide x 1.11 + ferric oxide

Fig. 3. Weight percent SiO_2 by energy dispersive analysis versus chemical analysis. (A) Individual values obtained by energy dispersive analysis. (B) Average values of individual values obtained by energy dispersive analysis.

over an extremely wide range. Although four kinds of chlorite having different chemical composition were examined with the transmission electron microscope, it was difficult to differentiate one species from another from their morphology or electron diffraction patterns.

Al-chlorite, Al-Mg-chlorite and Mg-chlorite have similar spectra differing only in the relative quantities of magnesium, aluminum, silicon and iron. However, these chlorites may be differentiated from each other on the basis of Mg-Al-Si ratios. Fe-chlorite, on the other hand, differs significantly from the others due to the presence of a magnesium peak and large iron peak.

Semiquantitative determination of chemical compositions

The incident electron beam on a specimen generates characteristic X-rays of elements present in the specimen. The intensity of the generated X-rays is indicated by the following equation: $I = K\rho W$; where K is a constant, ρ is the incident beam intensity, and W is the mass of the element in the irradiated area. In electron microprobe analysis of a thin film, the correction value for X-ray intensity is negligibly small, when the incident electron beam is focusable on a very small area. The analytical electron microscope is capable of acquiring an X-ray spectrum from particles less than 200 Å in diameter in approximately 100 seconds. Marshall and Hall (1968) reported in their electron microprobe analysis of thin films that the concentration of an element can be obtained by measuring its characteristic X-ray intensity, and simultaneously, the intensity of a portion of the continuous X-ray spectrum. Consequently, the ratio of characteristic X-ray intensity to continuum

X-ray intensity provides a measure of the concentration of an element which is independent of the thickness of the specimen.

In this study, the relative peak intensity ratio of each element was calculated from the following equation, with the total X-ray intensity in the specified X-ray energy range between 0 keV and 8 keV, as constant.

$$n_{11}Na + n_{12}Mg + \cdots + n_jX_j + \cdots + n_{92}U$$
$$= K \text{ (constant)}$$

where n_j is the ratio of a net peak intensity obtained by subtracting the background intensity, to the total X-ray intensity. X-ray intensities and background intensities were measured more than 5 times for each specimen. The duration of measuring X-ray intensity was 100–200 seconds per position. The numerical value of K varies with each specimen. The value of K in a given specimen was obtained after subtracting the water content [H_2O (+) and H_2O (−)] from the total obtained by ordinary chemical analysis. Table 2 compares the average peak intensity ratios n_j of 21 minerals and the values obtained from chemical analysis.

DISCUSSION

The characteristic X-ray intensity for a given element in a sample is only roughly proportional to the concentration of the element. The intensity is significantly affected by both instrumental and physical factors. The effect of the instrumental factors include the X-ray detection efficiency and the electron beam potential and current. These effects of instrumental variables can be minimized with the ratio of the measured intensities of the elements in the sample to those in standards of
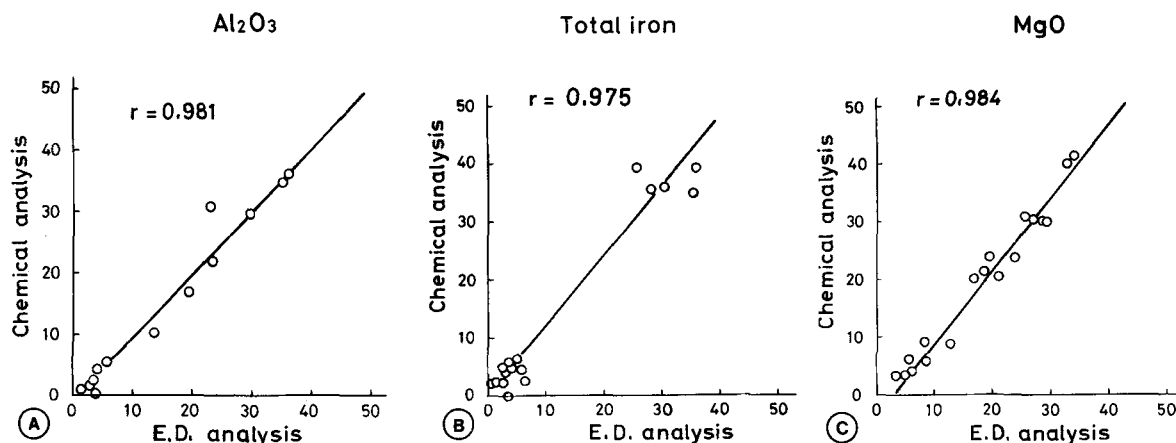
Fig. 4. Weight percent Al_2O_3 (A), total iron (B) and MgO (C) by energy dispersive analysis versus chemical analysis.

known composition. The physical factors are dependent on the sample composition and include the atomic number, absorption and secondary fluorescent effects. Correction for the atomic number, absorption and fluorescence effects have been developed and are widely used for thick polished specimens. Recently Waldl et al. (1975) described an empirical method for energy dispersive X-ray microanalysis of ternary and multicomponent alloy systems. They have introduced the following intensity reduction to eliminate the influence of instrumental fluctuations.

$$K_i^{red} = \frac{I_i}{I_t} = \frac{I_i}{\sum_i I_t + I_b}$$

where I_i is the intensity of the X-ray peak of an element i, I_t is the total measured intensity and I_b is the background intensity.

In the case of very thin specimens, as used for the transmission electron microscope, however, the analytical technique for bulk specimens cannot be employed simply. Several techniques have been developed primarily for the quantitative determination of elemental concentration in ultrathin specimens (Marshall and Hall, 1968; Namae, 1975; Chandler and Morton, 1976). Marshall and Hall (1968) showed the concentration of an element could be determined by the ratio of the intensity of the characteristic line to that of the continuous radiation from the same analyzing point. The method proposed by Namae (1975) is simple and useful for a very thin specimen, without knowing the thickness of the specimens, when the constant K of an element is already determined. However, it is difficult to prepare the specimens in the same thickness as the standard, and to determine the constant K of each element in specimens. Since the specimens used in this study are thin enough for use with a conventional 100 kV transmission electron microscope, the activated volume by the incident electron beam is very small

compared to the bulk specimen. Furthermore they are transparent to most of the primary X-rays produced by incident electron beam. Hence the matrix effects on characteristic X-rays (atomic number effect, absorption effect and fluorescence effect) can be neglected. In this study the ratio of the characteristic X-ray intensity of an element to the sum of the intensities of all of the elements in the sample is taken as a measure of concentration of that element. The SiO_2 content calculated this way is plotted against the value obtained by chemical analysis in Figure 3A. The average value of individual SiO_2 content for each specimen is plotted in Figure 3B, in relation to the chemical values. Highly significant regression was obtained in both cases;

Y = 0.90X + 2.685	from Figure 3A
Y = 0.95X + 0.241	from Figure 3B

These regressions have correlation constants of r = 0.949 and r = 0.973, respectively. Figures 4A,B and C show the energy dispersive results for Al_2O_3, total iron and MgO versus the values obtained by chemical analysis. A linear regression analysis calculated for Al_2O_3, total iron and MgO gave the following results. Correlation coefficients are higher than 0.97.

Al_2O_3:	Y = 1.06X − 1.35	r = 0.981
Total iron:	Y = 1.17X + 0.03	r = 0.975
MgO:	Y = 1.21X − 2.46	r = 0.984

There is a little lower energy dispersive value for total iron and MgO compared to the chemical data. Generally energy dispersive results are comparable with those obtained by chemical analysis.

The procedure described here can omit the process of estimating thickness of each specimen and determining the constant K for each element in the specimens. Furthermore, using this method a good correlation is obtained between the energy dispersive and chemical determination for SiO_2, Al_2O_3, total iron and
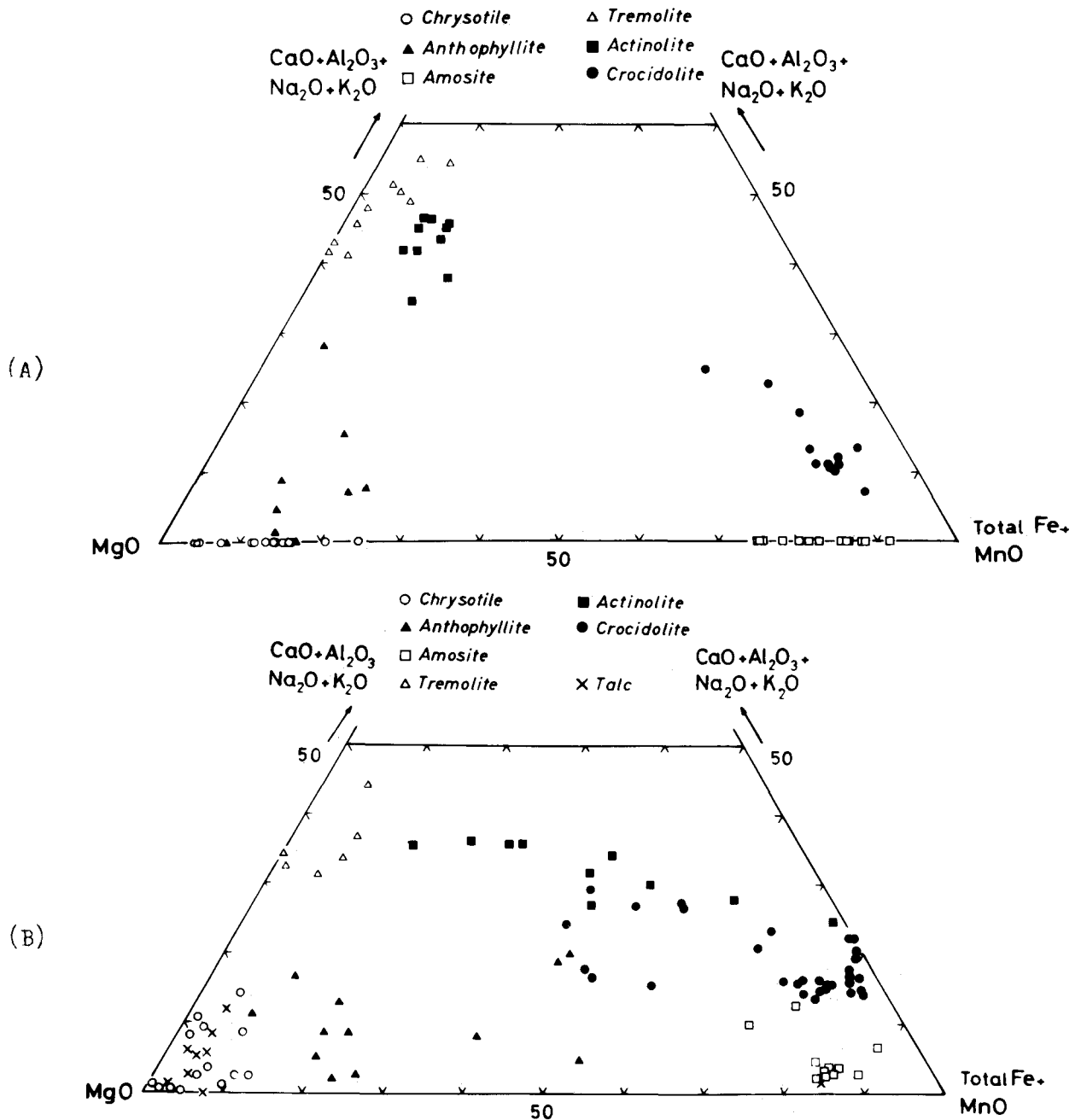
Fig. 5. Diagrams of three component composition fields for asbestos and talc. (A) Energy dispersive results of this study. (B) Chemical analytical data quoted from several researchers.

MgO, which are major components of silicate minerals. The principal feature of this method lies in its rapidity and the good results. Hence, application of this method is considered to be eminently satisfactory for many purposes, such as characterization of asbestos in environmental and tissue samples.

REFERENCES

Chandler, J. A. and Morton, M. S. (1976) Determination of elemental area concentration in ultrathin specimen by X-ray microanalysis and atomic absorption spectrometry: *Anal. Chem.* **48,** 1316–1318.

Henderson, W. J., Chandler, J. A., Blundell, G., Griffiths, C. and Dav-

ies, J. (1973) The application of analytical electron microscopy to the study of diseased biological tissue: *J. Microsc.* **99**, 183–192.

Kramer, J. R. (1976) Fibrous cummingtonite in Lake Superior: *Can. Mineral.* **14**, 91–98.

Langer, A. M., Selikoff, I. J. and Sastre, A. (1971) Chrysotile asbestos in the lungs of persons in New York City: *Arch. Environ. Health* **22**, 348–361.

Langer, A. M., Mackler, A. D. and Pooley, F. D. (1974) Electron microscopical investigation of asbestos fibers: *Environ. Health Perspect.* **9**, 63–80.

Marshall, D. J. and Hall, T. A. (1968) Electron-probe X-ray microanalysis of thin films: *Br. J. Appl. Phys.* Ser. 2, **1**, 1651–1656.

Namae, T. (1975) A method of quantitative analysis for thin specimens by energy dispersive spectrometer fitted to transmission electron microscope: *J. Electron Microsc.* **24**, 1–6.

Nicholson, W. J. (1974) Analysis of amphibole asbestiform fibers in municipal water supplies: *Environ. Health Perspect.* **9**, 165–172.

Pooley, F. D. (1972) Electron microscope characteristics of inhaled chrysotile asbestos fibre: *Br. J. Ind. Med.* **29**, 146–153.

Pooley, F. D. (1976) An examination of the fibrous mineral content of asbestos lung tissue from the Canadian chrysotile mining industry: *Environ. Res.* **12**, 281–298.

Rubin, I. B. and Maggiore, C. J. (1974) Elemental analysis of asbestos fibers by means of electron probe technique: *Environ. Health Perspect.* **9**, 81–94.

Selikoff, I. J. (1972) Carcinogenicity of amosite asbestos: *Arch. Environ. Health* **25**, 183–188.

Waldl, E., Walfermann, H., Ruscovic, N. and Warlimont, H. (1975) High-accuracy, empirical method of quantitative electron microprobe analysis using an energy dispersive system: *Anal. Chem.* **47**, 1017–1019.

Резюме- С помощью трансмиссионного электронного микроскопа,оборудованного рассеивающим энергию спектрометром,стало возможным определять морфологические,структурные и химические характеристики отдельных асбестовых волокон и глинистых минералов без повторной центровки оборудования. Приводятся данные анализов 21 водных силикатов,асбестов и глинистых минералов,полученных с помощью обычных химических и рассеивающих энергию методов. Результаты использования рассеивающих энергию методов были сопоставимы с результатами химических анализов.Применение этой процедуры для изучения асбестовых волокон доказало его практичность и пригодность для получения характеристики асбестов в природных и тканевых образцах.

Kurzreferat- Indem ein Transmission-Elektronen-Mikroskop, ausgestattet mit einem Energie-Streuungsspektrometer, benutzt wurde, war es möglich, die mor-phologischen, strukturellen und chemischen Eigenschaften von einzelnen Asbestfasern und Tonmineralien zu ermitteln, ohne die Apparatur wieder zu eichen. Eine schnelle und bequeme Methode für semi-quantitative Analyse wird vogeschlagen. Analysenresultate, erhalten durch allgemeine, chemische und Energie-Streuungsmethoden, für 21 wasserhaltige Silikate, Asbest und Tonmineralien sind angegeben. Die Resultate der Energie-Streuungsmethode waren vergleichbar mit denen, erhalten durch chemische Analyse. Anwendung dieser Prozedur auf Asbestfasern, hat bewiesen,daß diese Methode praktisch und brauchbar für die Charakterisierung von Asbest in Umwelt-und Gewebeproben ist.

Résumé-Par l'emploi d'un microscope électronique à transmission équippé d'un spectromètre dispersant l'énergie,il a été possible de détecter les caractéristiques morphologiques,structurales et chimiques de fibres d'asbeste individuelles et de minéraux argileux sans réaligner l'équipement.Un procédé rapide et commode pour l'analyse semi-quantitative est proposé.Des analyses sont données pour 21 silicates hydratées,asbestes et mineraux argileux,à la fois par des méthodes chimiques ordinaires et des méthodes dispersant l'énergie.Les résultats des méthodes dispersant l'énergie sont comparables à ceux obtenus par analyse chimique.L'application de ce procédé aux fibres d'asbeste prouvent que cette méthode est pratique et valable pour la caractérisation d'asbeste dans les échantillons de tissu et du milieu ambiant.